Calix[4]arene-based metal-organic frameworks: towards hierarchically porous materials

Sean P. Bew,* Andrew D. Burrows,* Tina Düren,* Mary F. Mahon,

Peyman Z. Moghadam, Viorica M. Sebestyen and Sean Thurston

Supplementary information

Synthetic details

General details

25,26,27,28-Tetrakis(1-propoxy)calix[4]arene-5,17-dicarboxylic acid (H_2caldc) was prepared by the previously reported method.[S1] All other reagents were purchased commercially and used without further purification.

Powder X-ray powder diffractions (PXRDs) were recorded at the University of Bath on a Bruker AXS D8 Advance diffractometer with copper Kα radiation of wavelength 1.5406 Å at 298 K. Samples were placed in 0.5 mm diameter Lindemann capillaries, and measured with a 2θ range of 3-60°. The step size was 0.016° with time per step of 134.5 s. Simulated X-ray powder patterns were generated from single crystal data that were imported into PowderCell[S2] with the step size of 0.02° and time per step of 1.00 s.

X-ray single diffraction data for **1** and **3** were collected on a Nonius Kappa CCD diffractometer, whereas **4** was collected on an Oxford Diffraction Gemini diffractometer fitted with an Atlas CCD detector. In all cases, Mo-K_α radiation of wavelength 0.71073 Å was used and data collections were carried out at 150 K at the University of Bath.

TGA experiments were performed on a Perkin Elmer TGA 4000 Thermogravimetric Analyser at the University of Bath. The samples were heated from 45°C to 600°C at a heating rate of 10°C/min, under a flow of nitrogen (20 mL/min).

Synthesis of $[Cu_2(caldc)_2(DMF)_2]$ ***1***

A solution of $Cu(NO_3)_2\cdot 3H_2O$ (0.024 g, 0.10 mmol) in water (5 cm^3) was placed in a thick-walled glass vial, and a layer of DMF (5 cm^3) carefully placed on top of the solution. H_2caldc (0.068 g, 0.10 mmol) was dissolved in DMF (5 cm^3) then carefully layered on top of the DMF layer in the vial. The vial was transferred to an oven and heated at 80°C for three days. The resultant turquoise powder was separated by filtration, washed with DMF and air-dried. Yield 0.074 g, (90 %). The powder X-ray diffraction pattern (Figure S1) shows a good match with the powder pattern simulated from the X-ray crystal structure. Small blue plate-like crystals were harvested from a similar reaction using $CuCl_2$ instead of $Cu(NO_3)_2\cdot 3H_2O$ as the copper source, though the product in this case was not phase-pure. The thermogravimetric analysis for **1** is shown in Figure S2.

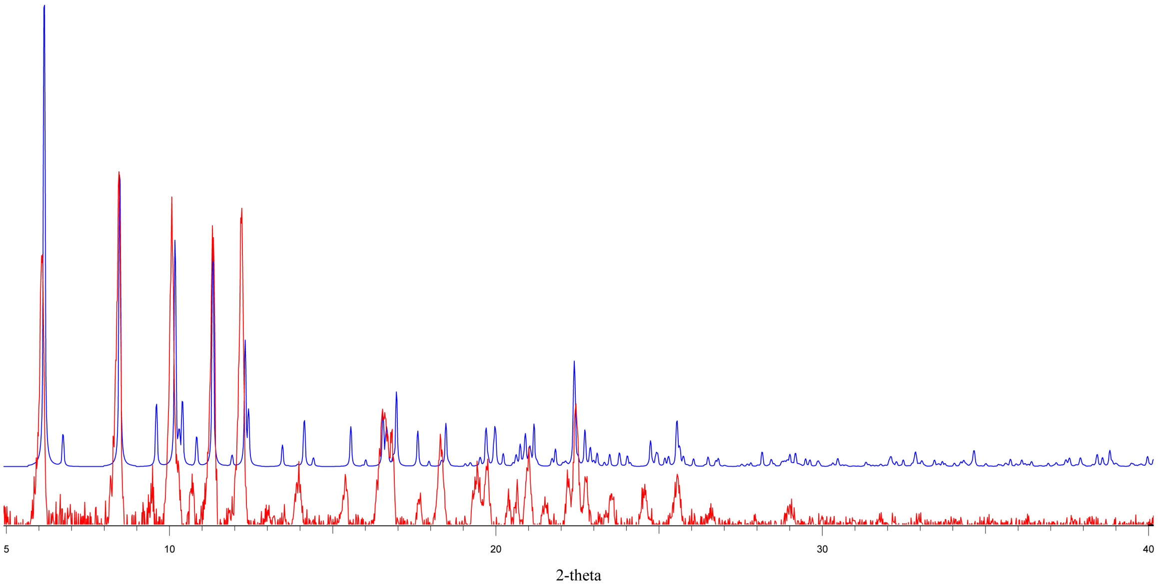

Fig. S1. The experimental powder X-ray diffraction pattern for [$Cu_2(caldc)_2(DMF)_2$] **1** (red) and that simulated from the crystal structure (blue).

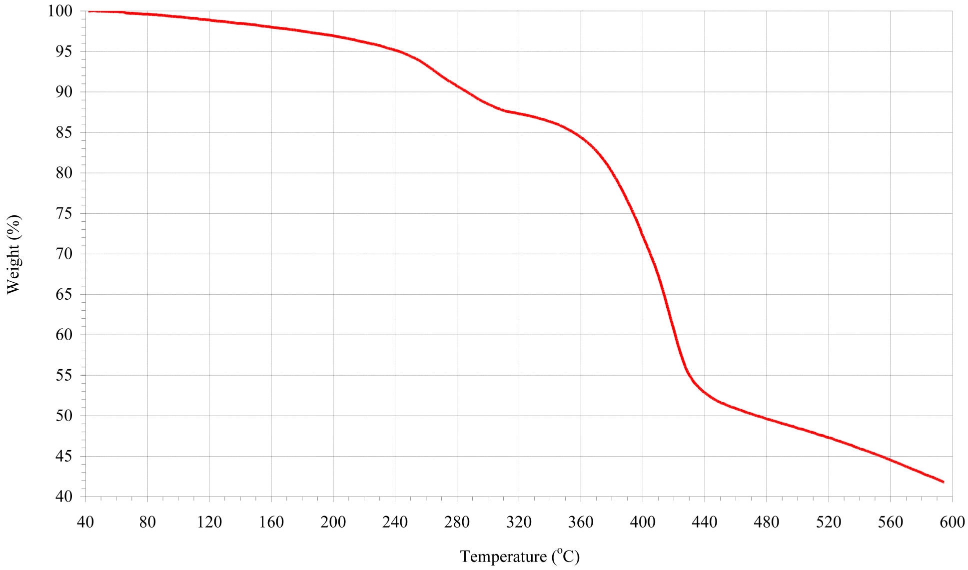

Fig. S2. The thermogravimetric analysis of [$Cu_2(caldc)_2(DMF)_2$] **1**.

Synthesis of [$Zn_2(caldc)_2(DMF)_2$] ***2***

H_2caldc (0.012 g, 0.018 mmol) and $Zn(OAc)_2 \cdot 2H_2O$ (0.002 g, 0.009 mmol) were dissolved in DMF (2 cm^3), and carefully placed on top of a layer of deionised water (1 cm^3) in a thick-walled glass vial. The vial was transferred to an oven and heated at 90°C for three days. The resultant small colourless crystals were separated by filtration, washed with DMF and air-dried. The powder X-ray diffraction pattern (Figure S3) shows that **2** is isostructural to **1**.

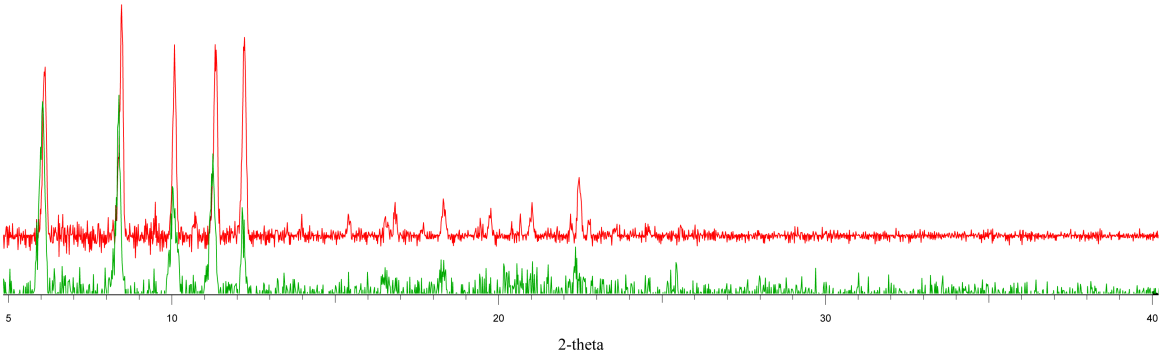

Fig. S3. The experimental powder X-ray diffraction pattern for $[Zn_2(caldc)_2(DMF)_2]$ **2** (green) and that for $[Cu_2(caldc)_2(DMF)_2]$ **1** (red).

Synthesis of $[Cd_2(caldc)_2(DMF)_2]\cdot 3DMF$ ***3***

In a thick-walled glass vial, a layer of DMF (3 cm^3) was added to a layer of deionized water (3 cm^3). A solution containing $Cd(NO_3)_2\cdot 4H_2O$ (0.031 g, 0.1 mmol) and H_2caldc (0.068 g, 0.1 mmol) in DMF (10 cm^3) was layered carefully by syringe on top of the DMF/water layers and the vial was capped with a lid. The mixture was heated in an oven at 80°C for three days. The resulting colourless needle-shaped crystals of **3** were separated by filtration, washed with DMF and air-dried. Yield 0.043 g (45 %). The powder X-ray diffraction pattern for **3** is shown in Figure S4 and the TGA is shown in Figure S5.

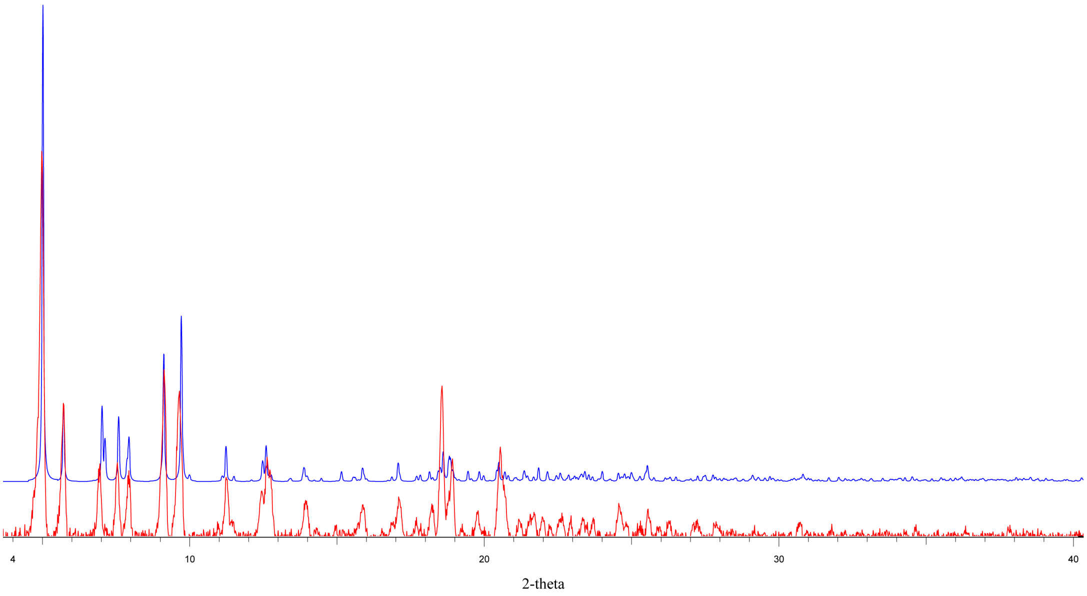

Fig. S4. The experimental powder X-ray diffraction pattern for $[Cd_2(caldc)_2(DMF)_2]\cdot 3DMF$ **3** (red) and that simulated from the crystal structure (blue).

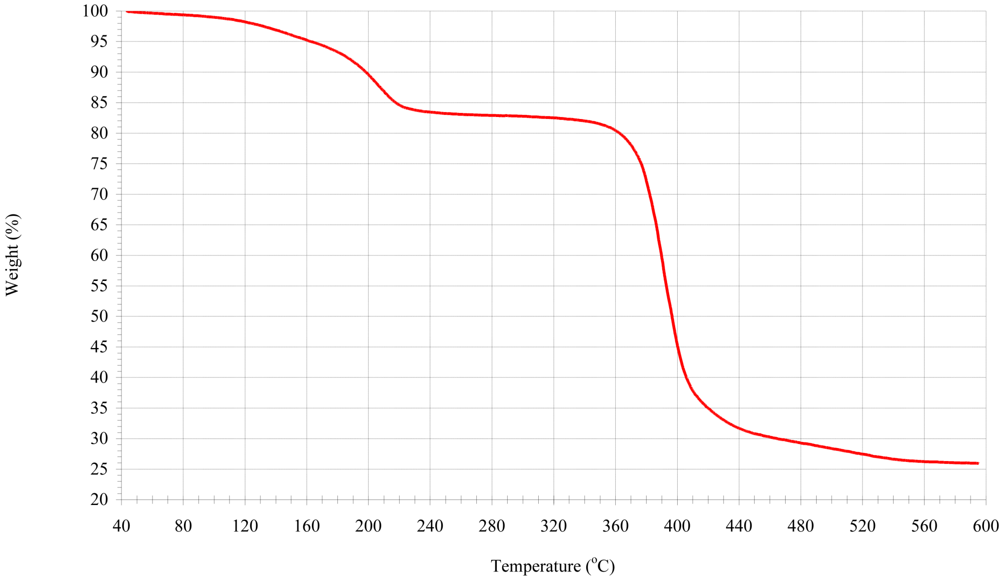

Fig. S5. The thermogravimetric analysis of [$Cd_2(caldc)_2(DMF)_2$]·3DMF **3**. The observed mass loss between room temperature and 280 °C corresponds to the loss of coordinated and unbound DMF (calc. 18.8%).

Synthesis of [$Co_5(caldc)_4(OH)_2(H_2O)_4$]·8DMF ***4***

A solution of $Co(NO_3)_2\cdot6H_2O$ (0.003 g, 0.009 mmol) and H_2caldc (0.012 g, 0.018 mmol) in DMF (2 cm^3) was carefully layered onto deionised water (1 cm^3) in a thick-walled glass vial and the mixture and heated at 90°C for three days. The resultant purple, block-shaped crystals of **4** were separated by filtration. The powder X-ray diffraction analysis (Figure S6) revealed that **4** is the major product, though it was not possible to separate **4** from a minor impurity.

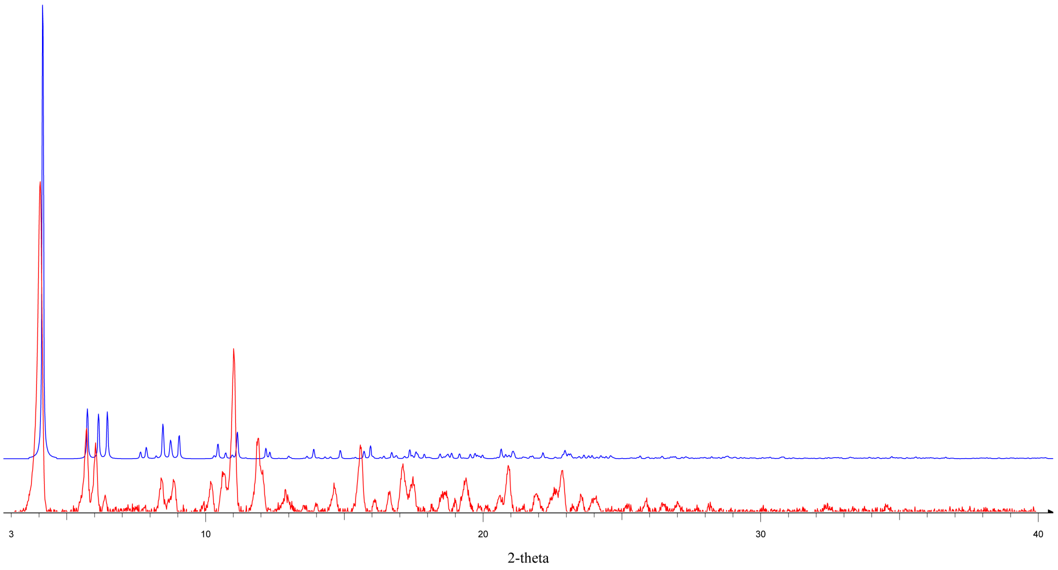

Fig. S6. The experimental powder X-ray diffraction pattern for [$Co_5(caldc)_4(OH)_2(H_2O)_4$]·8DMF **4** (red) and that simulated from the crystal structure (blue).

Table S1. Crystal data and structure refinement for **1**.

Empirical formula	$C_{90}H_{106}Cu_2N_2O_{18}$
Formula weight	1630.85
Temperature	150(2) K
Wavelength	0.71073 Å
Crystal system	Monoclinic
Space group	$P2_1/c$
Unit cell dimensions	a = 9.4670(2)Å α = 90°
	b = 26.3310(5)Å β = 102.789(1)°
	c = 17.6480(5)Å γ = 90°
Volume	4290.08(17) $Å^3$
Z	2
Density (calculated)	1.262 g cm^{-3}
Absorption coefficient	0.563 mm^{-1}
$F(000)$	1724
Crystal size	0.30 x 0.20 x 0.20 mm
Theta range for data collection	3.58 to 24.93°
Index ranges	$-11 \le h \le 11$; $-31 \le k \le 29$; $-20 \le l \le 20$
Reflections collected	47644
Independent reflections	7394 [R(int) = 0.1632]
Reflections observed (>2σ)	4673
Data Completeness	0.986
Absorption correction	Semi-empirical from equivalents
Max. and min. transmission	0.990 and 0.853
Refinement method	Full-matrix least-squares on F^2
Data / restraints / parameters	7394 / 42 / 537
Goodness-of-fit on F^2	1.018
Final R indices [$I > 2\sigma(I)$]	$R1$ = 0.0700 $wR2$ = 0.1644
R indices (all data)	$R1$ = 0.1265 $wR2$ = 0.1955
Largest diff. peak and hole	2.114 and -0.678 e$Å^{-3}$

Notes

The asymmetric unit consists of one copper centre, one DMF molecule, and one caldc dianion. Carbons 6-8 of the *n*-propoxy functionality are modeled as being disordered over two sites. This approach yielded the optimal convergence, but the disorder is somewhat smeared. Hence, C–C distance restraints and ADP restraints were applied to these partial occupancy carbon atoms.

The packing of the sheets is shown in Figure S7.

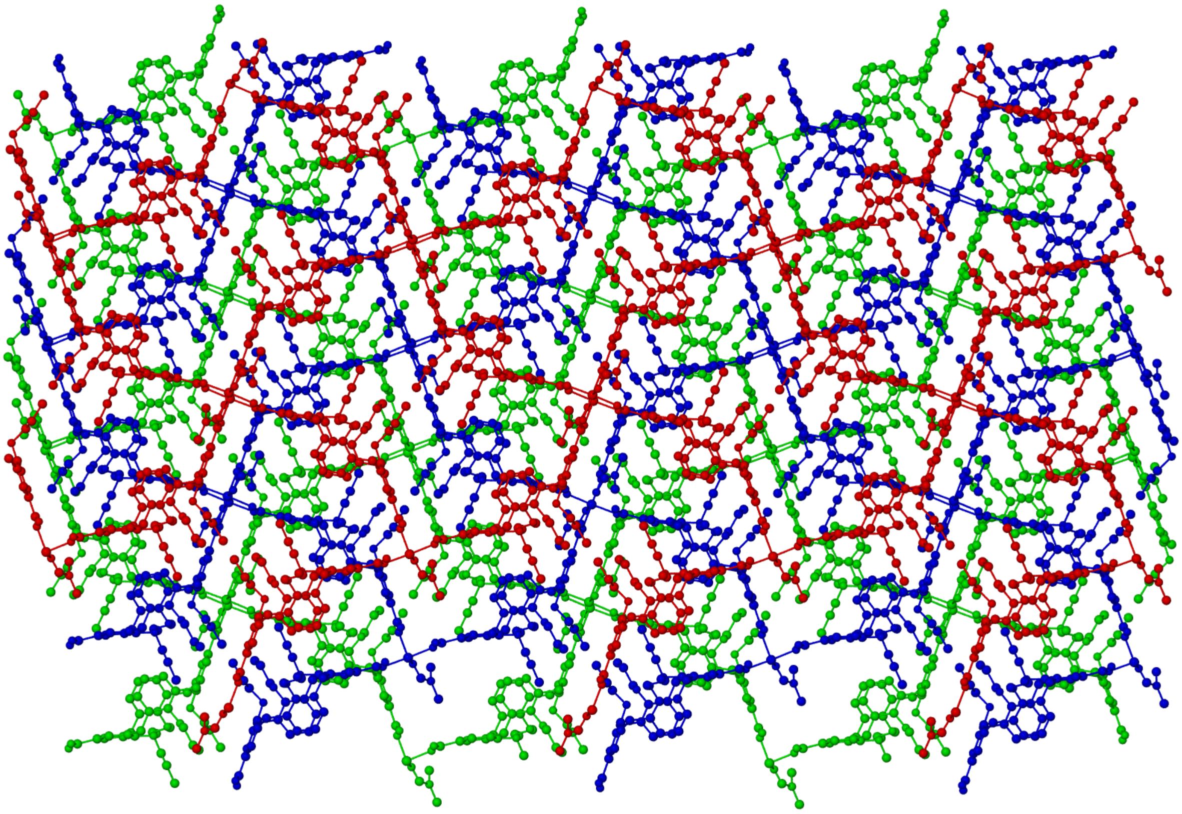

Fig. S7. The structure of [$Cu_2(caldc)_2(DMF)_2$] **1**, showing the manner in which the sheets stack together.

Table S2. Crystal data and structure refinement for **3**.

Empirical formula	$C_{99}H_{127}Cd_2N_5O_{21}$
Formula weight	1947.86
Temperature	150(2) K
Wavelength	0.71073 Å
Crystal system	Monoclinic
Space group	$P2_1/_n$
Unit cell dimensions	a = 15.5500(3)Å α = 90°
	b = 24.9210(2)Å β = 90.005(1)°
	c = 25.2820(4)Å γ = 90°
Volume	9797.3(3) Å^3
Z	4
Density (calculated)	1.321 g cm^{-3}
Absorption coefficient	0.505 mm^{-1}
F(000)	4080
Crystal size	0.50 x 0.13 x 0.13 mm
Theta range for data collection	3.59 to 25.03°
Index ranges	$-18 \leq h \leq 17$; $-29 \leq k \leq 29$; $-27 \leq l \leq 30$
Reflections collected	74270
Independent reflections	17143 [R(int) = 0.1147]
Reflections observed (>2σ)	12798
Data Completeness	0.991
Refinement method	Full-matrix least-squares on F^2
Data / restraints / parameters	17143 / 65 / 1111
Goodness-of-fit on F^2	1.083
Final R indices [$I > 2\sigma(I)$]	$R1$ = 0.0693 $wR2$ = 0.1999
R indices (all data)	$R1$ = 0.0885 $wR2$ = 0.2163
Largest diff. peak and hole	2.163 and –1.077 eÅ^{-3}

Notes

Several of the *n*-propyl groups appended to the calixarenes exhibited 60:40 disorder, as did the DMF moiety ligated to Cd(1). Only major atom fractions in these disordered moieties were refined anisotropically, with the exception of the group containing O(11), where the electron density was very smeared. O–C and C–C distance restraints were applied in disordered *n*-propyl functionalities to assist convergence.

There is also 'free' solvent in the asymmetric unit of this structure. This consists of one area of well defined solvent, and 2 areas where it is more diffuse. Strenuous efforts could not successfully render a credible model that would converge for the diffuse regions - which each approximated to one molecule of DMF. Hence, Platon SQUEEZE was employed, and this also suggested the presence of two molecules of DMF in terms of void volume. Data presented herein takes account of this 'pre-SQUEEZE' solvent.

Data were truncated to a maximum Bragg angle of 25^{o} for this needle-like crystal. A fall off in diffraction intensity was noted – probably a function of the disordered solvent present and the small size of two of the sample dimensions.

Table S3. Crystal data and structure refinement for **4**.

Empirical formula	$C_{96}H_{125}Co_{2.5}N_4O_{23}$
Formula weight	1850.32
Temperature	150(2) K
Wavelength	0.7107 Å
Crystal system	Triclinic
Space group	P–1
Unit cell dimensions	a = 13.7658(3)Å, α = 104.894(3)°
	b = 16.0409(5)Å, β = 89.547(3)°
	c = 22.3491(10)Å, γ = 92.223(2)°
Volume	4765.6(3) $Å^3$
Z	2
Density (calculated)	1.289 g cm^{-3}
Absorption coefficient	0.505 mm^{-1}
F(000)	1961
Crystal size	0.25 x 0.15 x 0.10 mm
Theta range for data collection	2.93 to 26.37°
Index ranges	$-17 \leq h \leq 17$; $-20 \leq k \leq 16$; $-27 \leq l \leq 27$
Reflections collected	31341
Independent reflections	18857 [R(int) = 0.0420]
Reflections observed (>2σ)	9096
Data Completeness	0.969
Absorption correction	Semi-empirical from equivalents
Max. and min. transmission	1.00000 and 0.84060
Refinement method	Full-matrix least-squares on F^2
Data / restraints / parameters	18857 / 98 / 1044
Goodness-of-fit on F^2	0.907
Final R indices [$I > 2\sigma(I)$]	$R1$ = 0.0775 $wR2$ = 0.2103
R indices (all data)	$R1$ = 0.1369 $wR2$ = 0.2299
Largest diff. peak and hole	1.523 and –0.536 $eÅ^{-3}$

Notes

Two data collections were required in order to get optimal data. The asymmetric unit contains 2.5 x cobalt centres (Co1 located at an inversion centre), 2 fully deprotonated calixarene dicarboxylate, 2 DMF molecules, and a mixture of oxygens/hydroxide anions (O1, O2 and O3). The core is well resolved, with the exception of the hydroxide/water hydrogens atoms. The latter could not be credibly located and hence were omitted from the refinement.

One of the DMF molecules exhibited disorder of 3 atoms therein – namely C89, C90 and C91– in a 50:50 ratio. The electron density is generally smeared in the calixarene pendant group regions. The extent of this smearing led to disorder modelling for C35, C36 and C42. Based on residual electron density and void volume calculations, it was evident that the lattice contained some diffuse solvent.

This has been included as 2 molecules of DMF per asymmetric unit following implementation of PLATON SQUEEZE.

A considerable number of distance restraints pertaining to the *n*-propoxy groups plus some ADP restraints were necessary in order to facilitate convergence of this structure.

Computational details

Adsorption of methane, hydrogen, and their mixtures in **1**, **3** and **4** were computed from using grand canonical Monte Carlo (GCMC) simulations[S3] implemented in the RASPA[S4] simulation package. In the grand canonical ensemble, the chemical potential, the volume, and the temperature are kept constant while the number of molecules is allowed to fluctuate mimicking the experimental situation. This is achieved by randomly inserting, deleting, and translating and in the case of non-spherical molecules such as hydrogen also rotating the molecules. For binary mixtures, identity swap moves were also used for faster equilibration times. For all pure component isotherms, 1×10^5 equilibration and 2×10^5 production cycles were used for each point whereas for mixtures as many as 3×10^5 cycles were used for each equilibration and production run. Here, a cycle is defined as one MC move per molecule. Each simulation cell consisted of eight (2 × 2 × 2) unit cells to allow for good statistics. We considered the MOFs as rigid and the framework atoms were kept fixed at their crystallographic positions.

The input fugacities for the GCMC simulations, which are related to the chemical potential by an equation of state, were calculated from the Peng-Robinson equation of state. All results are reported as absolute amount adsorbed. For the mixtures, we calculated the selectivity which is defined as:

$$S_{\mathrm{CH_4/H_2}} = \frac{x_{\mathrm{CH_4}} / x_{\mathrm{H_2}}}{y_{\mathrm{CH_4}} / y_{\mathrm{H_2}}}$$

where x_i denotes the mole fractions of the component i in the adsorbed phase and y_i the mole fraction in the gas phase.

For the calculation of both the guest-guest and the guest-framework interactions, the Lennard-Jones potential was used with a cut-off radius of 12.8 Å. The Lennard Jones (LJ) parameters for all the framework were taken from the Dreiding force field[S5] except for metal atoms which were taken from UFF force field.[S6] The potential parameters for methane were taken from Goodbody et al.[S7] In this model, the methane molecule is modelled as a single sphere. Hydrogen was modelled as a two site LJ molecule.[S8] The Lorenz-Berthelot mixing rules were used to calculate mixed LJ parameters. All electrostatic interactions between guests and guest-host molecules were neglected.

Pure component adsorption

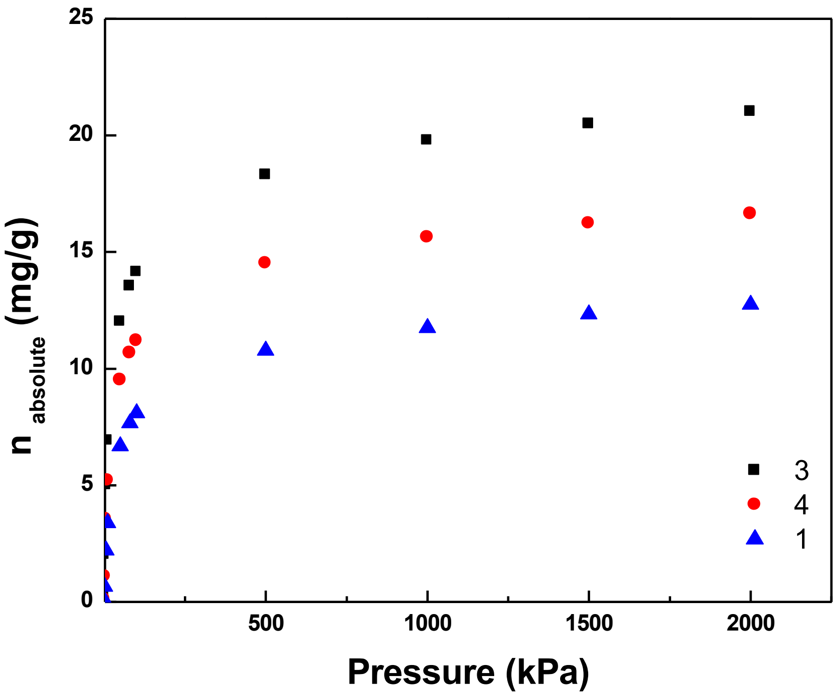

Fig. S8. Pure component adsorption isotherms for hydrogen at 77 K

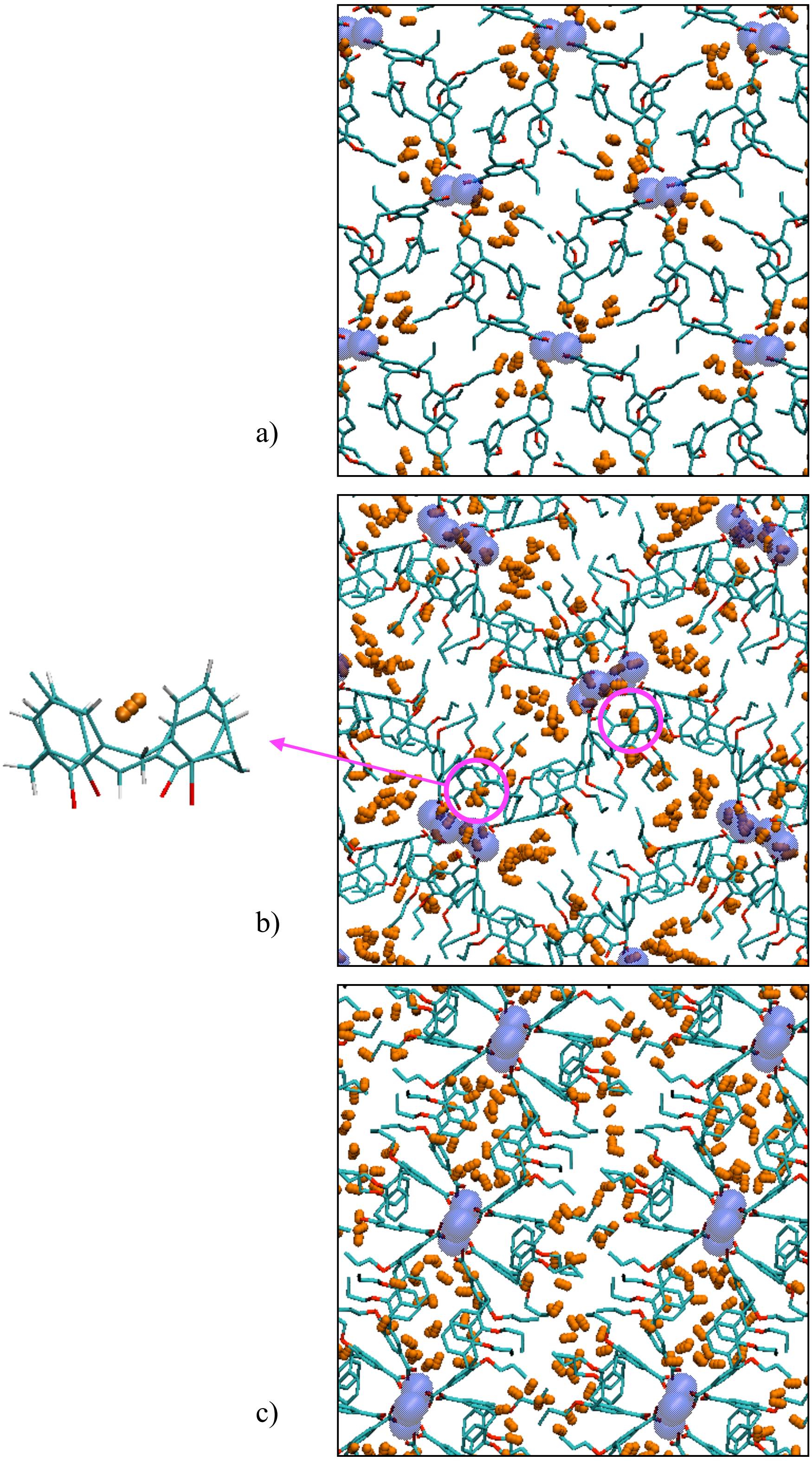

Fig. S9. Snapshots for hydrogen adsorbed in a) **1**, b) **3**, c) **4** at 20 bar and 77 K. Hydrogen is represented by orange spheres, metal clusters are shown in transparent blue spheres. Note that in only for **3** is the calix[4]arene bowl accessible to hydrogen as illustrated by the pink circles.

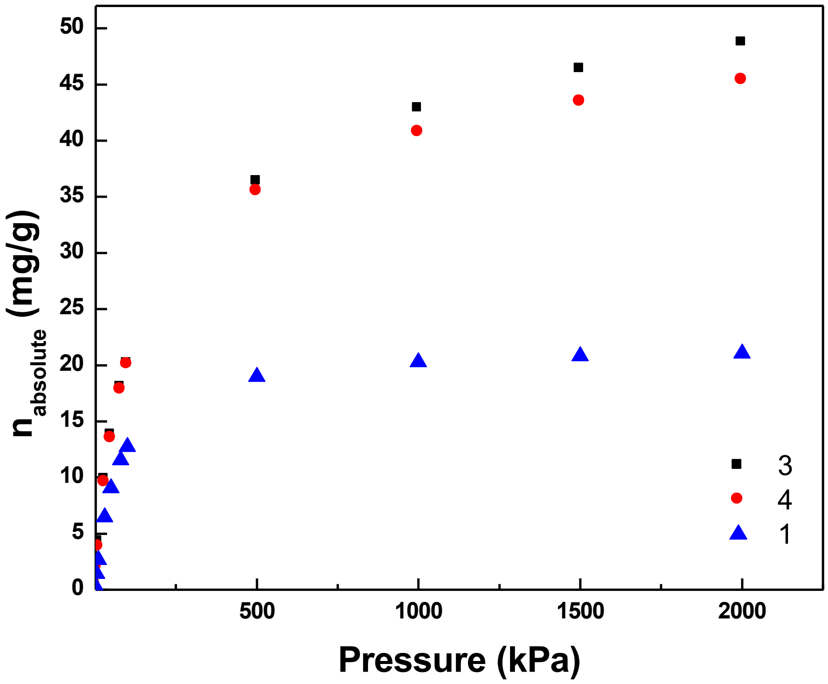

Fig. S10. Pure component adsorption isotherms for methane at 300 K

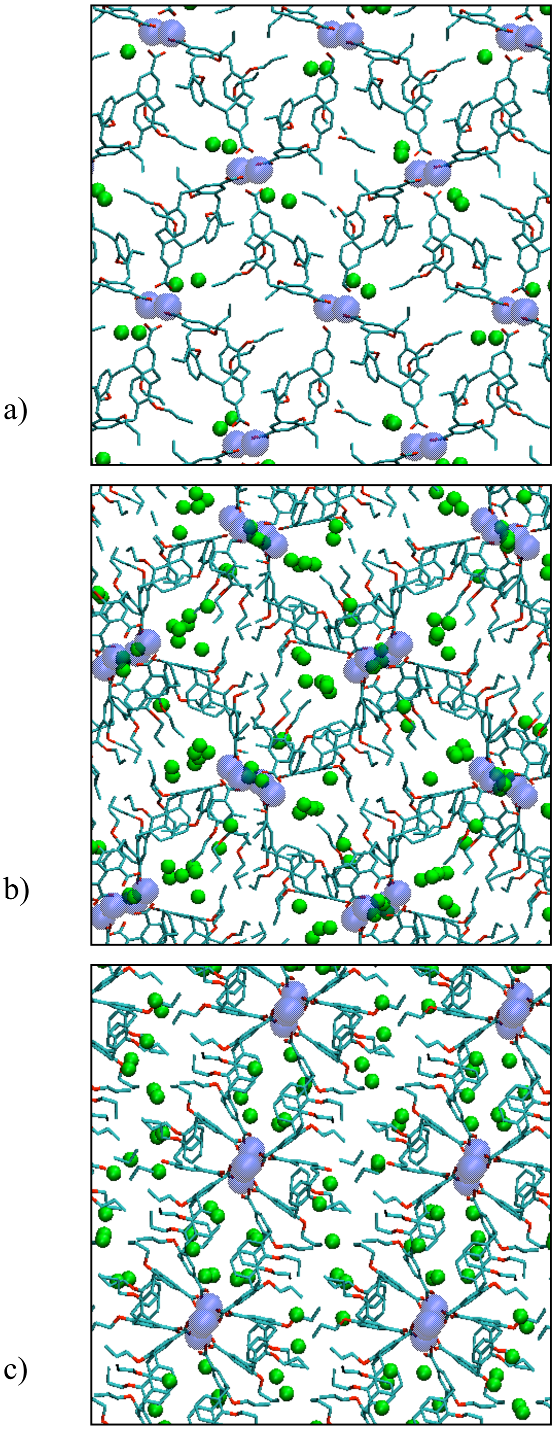

Fig. S11. Snapshots for methane adsorbed in a) **1**, b) **3**, c) **4** at 20 bar and 300 K. The green methane molecules are shown in spacefill representation, metal clusters are shown in transparent blue spheres. Note that in all three cases, the calix[4]arene bowls are inaccessible to methane.

Mixture adsorption

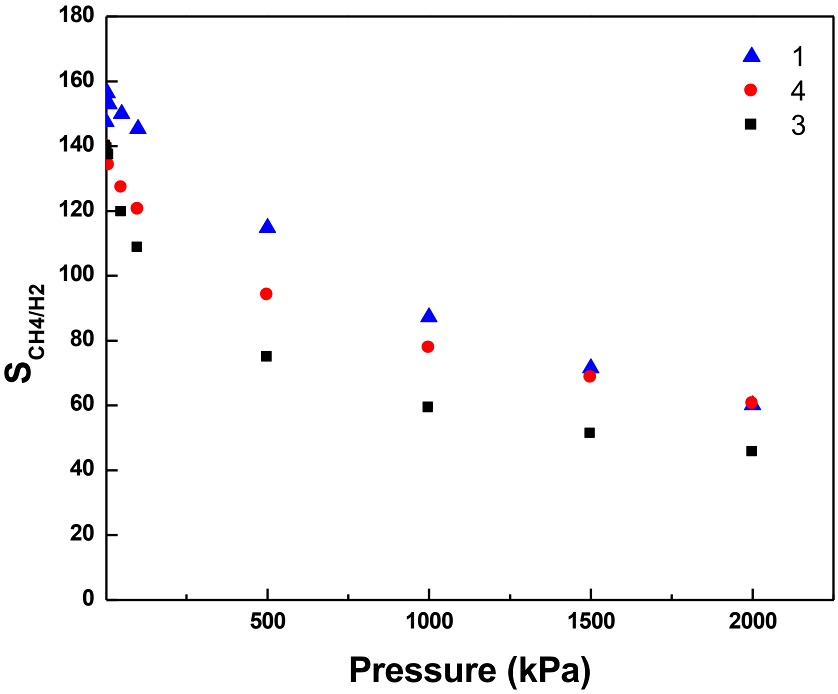

Fig. S12. Adsorption selectivity for CH_4 over H_2 at 300 K for an equimolar mixture of methane and hydrogen.

References

S1. W. Verboom, S. Datta, Z. Asfari, S. Harkema and D. N. Reinhoudt, *J. Org. Chem.*, 1992, **57**, 5394; B. R. Travis, M. Sivakumar, G. O. Hollist and B. Borhan, *Org. Lett.*, 2003, **5**, 1031.

S2. W. Kraus and G. Nolze, PowderCell for Windows 2.4, Federal Institute for Materials Research and Testing Rudower Chaussee 5, Berlin, Germany, 1999.

S3. D. Frenkel and B. Smit, *Understanding molecular simulation: from algorithms to applications*, Academic Press, 2002,

S4. D. Dubbeldam, S. Calero, D. E. Ellis and R. Q. Snurr, RASPA 1.0, Northwestern University, Evanston, IL, 2008.

S5. S. L. Mayo, B. D. Olafson and W. A. Goddard, *J. Phys. Chem.*, 1990, **94**, 8897.

S6. A. K. Rappe, C. J. Casewit, K. S. Colwell, W. A. Goddard and W. M. Skiff, *J. Am. Chem. Soc.*, 1992, **114**, 10024.

S7. S. J. Goodbody, K. Watanabe, D. MacGowan, J. P. R. B. Walton and N. Quirke, *J. Chem. Soc., Faraday Trans.*, 1991, **87**, 1951.

S8. Q. Yang and C. Zhong, *J. Phys. Chem. B*, 2005, **109**, 11862.